Glassy thermal conductivity in the two-phase $Cu_xAg_{3-x}SbSeTe_2$ alloy and high temperature thermoelectric behavior



2010 J. Phys.: Condens. Matter 22 035801

(http://iopscience.iop.org/0953-8984/22/3/035801)

J. Phys.: Condens. Matter **22** (2010) 035801 (5pp) doi:10.1088/0953-8984/22/3/035801

# Glassy thermal conductivity in the two-phase $Cu_xAg_{3-x}SbSeTe_2$ alloy and high temperature thermoelectric behavior

**F Drymiotis[1], T Drye[1], D Rhodes[1], Q Zhang[1], J C Lashey[2], Y Wang[1], S Cawthorne[1], B Ma[1], S Lindsey[1] and T Tritt[1]**

[1] Department of Physics and Astronomy, Clemson University, Clemson, SC 29634, USA
[2] Los Alamos National Laboratory, Los Alamos, NM 87545, USA

Received 16 November 2009, in final form 19 November 2009
Published 16 December 2009
Online at stacks.iop.org/JPhysCM/22/035801

**Abstract**

We have measured the thermal transport properties over the temperature range 1.8 K $< T <$ 700 K of a two-phase alloy synthesized by reacting $AgSbTe_2$ and $Ag_2Se$ in a 1:1 molar ratio. Typical electrical resistivity values at 700 K are in the range $\sim$4 m$\Omega$ cm $\leqslant \rho \leqslant$ 20 m$\Omega$ cm, while low thermal conductivity values ($\kappa < 1$ W m$^{-1}$ K$^{-1}$) were obtained. We find that the thermal conductivity of this crystalline alloy has a temperature dependence strikingly similar to those of amorphous solids. In addition the thermal conductivity, thermopower, and electrical resistivity decouple. This result makes it possible to optimize thermoelectric performance by minimizing the electrical resistivity. It is therefore envisaged that this system has potential as a high performance bulk thermoelectric.

## 1. Introduction

Sustainable energy research is currently on the forefront of scientific exploration thus a major effort is devoted to the development of new energy conservation and production techniques. Thermoelectric materials can play a significant role both in energy conservation and energy production, since they can convert wasted heat to useful electrical energy [1–3]. In automotive applications, thermoelectrics can be used to collect the wasted heat from the exhaust and return it to the vehicle, in order to power electrical components, thus removing engine load and decreasing consumption. Alternatively, hot-springs may be used to generate electrical power since they provide a natural temperature reservoir. For power generation applications, the dimensionless figure of merit $ZT$ (defined as $\alpha^2 T/\kappa\rho$ where $\alpha$ is the thermopower or Seebeck coefficient, $\rho$ is the electrical resistivity and $\kappa$ is the total thermal conductivity) should have its maximum value at temperatures at or above 400 °C. Very high values of $ZT$ ($>$2) have been observed in thin films [4] but unfortunately thin films are not suitable for high temperature and large scale applications. Thus, the current challenge is achieving comparable values of $ZT$ ($>$2) in bulk thermoelectric materials.

Synthesis of low carrier concentration complex alloys appears to be the most promising path for discovering new highly efficient bulk thermoelectric materials [5]. Complicated structures with large and complex unit cells give rise to low thermal conductivity. In addition the structural disorder may be manipulated in order to vary the values of the electrical resistivity and thermopower. An ideal scenario would be the formation of a complex alloy which behaves as phonon glass electron crystal (PGEC) [6] (i.e., an alloy which has the electronic properties of a crystalline system and the thermal transport behavior of a glass). Formation of complex multi-phase alloys is thus an intriguing and logical synthesis technique for generating a PGEC alloy. Depending on the relative volume of the phases, the disorder scale can be comparable to the wavelength of low wavelength phonons, consequently leading to low thermal conductivity. The main problem of this approach is the effect of the disorder on the electrical resistivity. Large electrical resistivity values will diminish thermoelectric performance so the challenge is determining the proper phases to be used in the synthesis of such a multi-phase alloy.

In this work we show that the two-phase alloy formed by melting $AgSbTe_2$–$Ag_2Se$ in a 1:1 molar ratio ($Ag_3SbSeTe_2$), is a PGEC material with the potential for very high thermoelectric performance. Both $AgSbTe_2$ and $Ag_2Se$ are well known thermoelectric materials [7–14] but most importantly they both have low thermal conductivity. The resulting two-phase alloy has good electronic properties but most notably its thermal

 

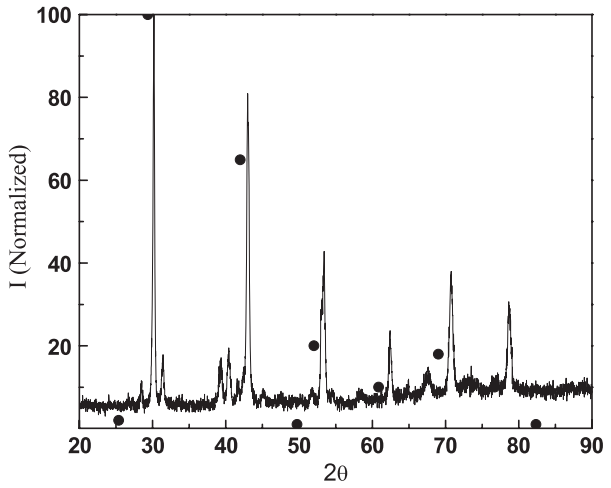


**Figure 1.** X-ray diffraction data of $Cu_{0.2}Ag_{2.8}SbSeTe_2$. The dark circles correspond to the location of the $AgSbTe_2$ peaks.

conductivity behavior is similar to the thermal conductivity behavior of amorphous materials.

## 2. Experiment

Ag, Cu, Sb, Te, Se with respective purities of 99.9999%, 99.9999%, 99.9999%, 99.9999% and 99.999% were placed in quartz tubes in stoichiometric ratios 3—$x$:$x$:2:1, with $x = 0, 0.1, 0.2$. The quartz tubes were then evacuated, sealed, and placed inside a box furnace. The samples were subsequently heated to 1000 °C where they were allowed to remain for 4 h, before finally being allowed to cool down to 500 °C at a rate of 10 °C $h^{-1}$, at which point the power to the furnace was turned off. The formed ingots were then removed from the quartz tubes and processed for measurement. The mass of each ingot was approximately 20 g. All samples obtained were highly dense with good mechanical properties. The density of all samples was approximately $d \sim 7.3$ g $cm^{-3}$.

The x-ray diffraction data was obtained using a commercial Rigaku® diffractometer and the SEM and EDX analysis were performed using the Hitachi S3400-N SEM. The high temperature resistivity and thermopower data were obtained using the ULVAC-ZEM2® measuring system. The high temperature thermal conductivity values were deduced from the thermal diffusivity values obtained using the Netzsch LFA 457® laser flash apparatus using the relation $\kappa = \alpha d C_P$, with $\alpha$ being the measured value of the thermal diffusivity, $d$ the density and $C_P$ the isobaric heat capacity. The value of $d$ used in the calculations was the measured density at room temperature, and the value of $C_P$ was taken to be the value of the Dulong–Petit limit. The low temperature thermal conductivity data was taken using a Quantum Design PPMS®.

## 3. Results and discussion

The x-ray diffraction data shows the presence of two distinct phases, a phase which crystallizes in the $AgSbTe_2$ rocksalt structure [12] ($cF8$, No 225) and a phase which crystallizes in the monoclinic $\alpha$-$Ag_2Te$ structure [15] ($mP12$, No 14) (figure 1). The crystal structure of these two phases is illustrated in figure 2. The average density of the samples is $d = 7.30$ g $cm^{-3}$ which is considerably higher than the density of $AgSbSe_2$ ($d = 6.69$ g $cm^{-3}$), slightly higher than the density of $AgSbTe_2$ ($d = 7.12$ g $cm^{-3}$) and significantly lower than the density of $\alpha$-$Ag_2Te$ ($d = 8.21$ g $cm^{-3}$).

The lattice parameter obtained from the x-ray (figure 1) data for the rocksalt phase is $a \sim 5.94$ A which lies between the lattice parameter of $AgSbSe_2$ ($a = 5.79$ A) and the lattice parameter of $AgSbTe_2$ ($a = 6.07$ A). Based on these parameters it appears that the composition of the resulting mixture is Se-doped $AgSbTe_2$ and Se-doped-$\alpha$-$Ag_2Te$. Preliminary EDX on different areas of the Cu-doped sample with distinct features, confirmed the existence of both Se-doped $AgSbTe_2$ and Se-doped monoclinic $Ag_2Te$. The result is not surprising since it has been shown that $Ag_2Te$ precipitates out of $AgSbTe_2$ during solidification [16], which implies that the monoclinic $Ag_2Te$, and not the orthorhombic $Ag_2Se$, is the thermodynamically stable second phase. Images of the phase reveal, as expected, two different phases which are additionally uniformly distributed. The phase separation between the rocksalt structure (dark shade) and the monoclinic structure (light shade) is distinct and micro-fractures can been seen at the phase boundaries shown in figure 3. Both phases seem to occupy the same volume.

Figure 4 shows that the temperature dependence of the electrical resistivity is typical of some type of an activated

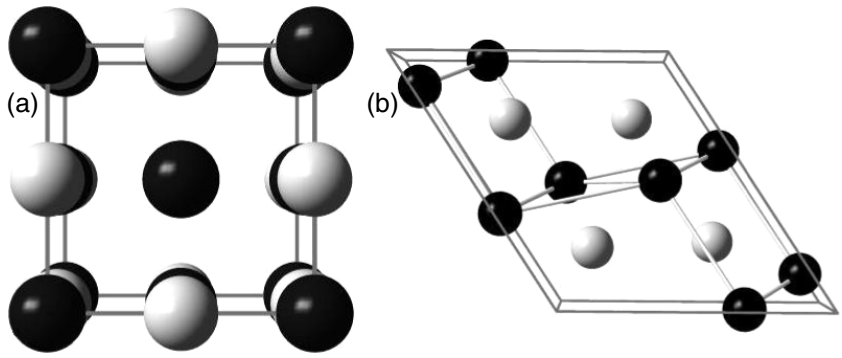


**Figure 2.** The (a) rocksalt $AgSbTe_2$ structure and (b) the monoclinic $Ag_2Te$ structure (index vector 0 1 0). Dark spheres correspond to Ag and Sb locations and gray spheres correspond to Te locations.

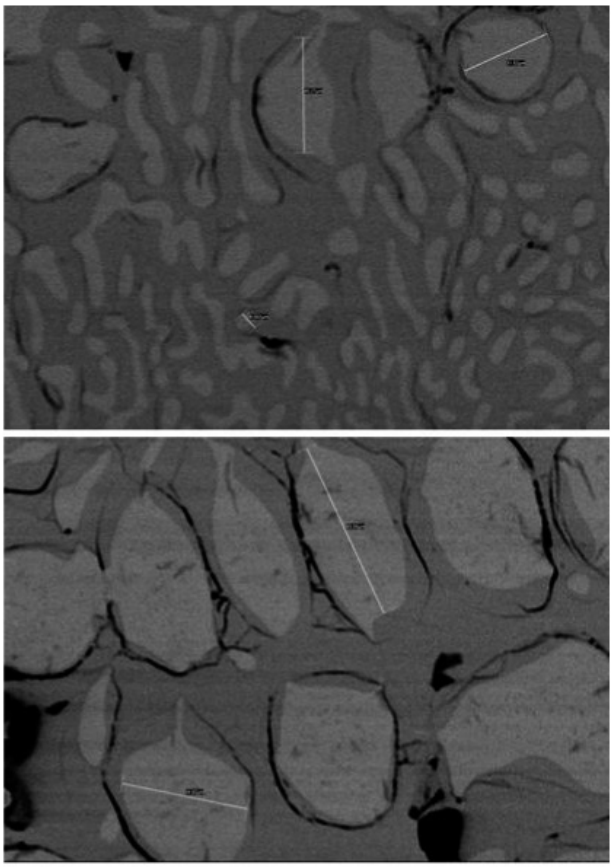

**Figure 3.** SEM image (top) shows the presence of both the cubic $AgSbTe_2$ (dark shade) and monoclinic $Ag_2Te$ (light shade). Close up (bottom) shows the micro-cracks which develop along the phase boundaries. The length scale associated with the $Ag_2Te$ region (light shade) is of tens of micrometers.

process. Activated behavior is observed at high temperatures while the room temperature resistivity is dominated by intrinsic effects. The feature at 400 K in the resistivity versus temperature data corresponds to the $\alpha \rightarrow \beta$ structural phase transition in the doped $Ag_2Te$. The resistivity decreases with increasing Cu concentration from a value of 11.8 m$\Omega$ cm for the $x = 0$ sample to 3.3 m$\Omega$ cm for the best $\delta = 0.2$ sample. The resistivity values vary from sample to sample which is expected behavior in a complex alloy with low electronic energies.

The cooling profile, sample homogeneity and variations in stoichiometry, and the presence of micro-fractures are all factors which can substantially affect electronic transport. We should note that in the samples not containing Cu, the resistivity and thermopower values change when the sample is annealed at 400 °C. Adding Cu stabilizes the resulting structure and consequently eliminates the changes in the electrical transport and thermopower behavior caused by annealing.

In contrast to the resistivity, the thermopower of the stoichiometric and Cu-doped samples is extremely robust and does not vary significantly from sample to sample as shown in figure 5. The thermopower shows n-type behavior at low temperatures and p-type behavior at high temperatures.

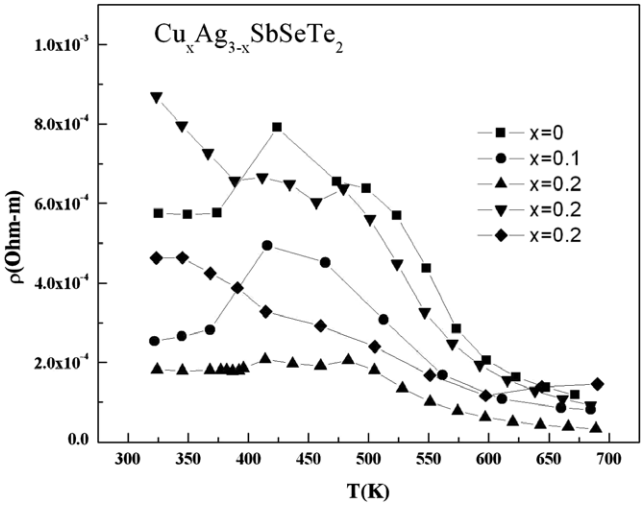


**Figure 4.** Electrical resistivity versus temperature of $Cu_xAg_{3-x}SbSeTe_2$ for $x = 0$, 0.1 and 0.2.

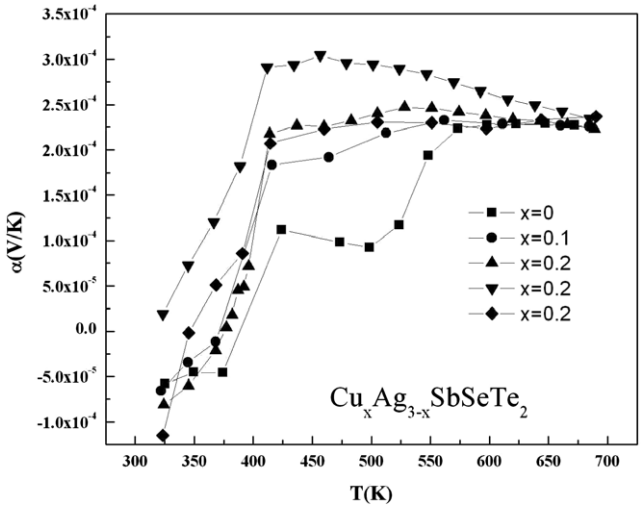


**Figure 5.** Thermopower versus temperature of $Cu_xAg_{3-x}SbSeTe_2$ for $x = 0$, 0.1 and 0.2.

The transition from n- to p-type behavior coincides with the $Ag_2Te$ $\alpha \rightarrow \beta$ structural phase transition. The value of the thermopower at 700 K is approximately $\alpha \sim 230\ \mu V\ K^{-1}$ for all samples. Cu doping does not produce significant changes in the thermopower which implies that Cu doping does not noticeably affect the band structure. This is not unexpected as Cu and Ag are isoelectronic. The most plausible explanation for this behavior is the presence of the observed micro-fractures. The concentration of micro-structures will presumably vary from sample to sample but it will have no effect on the thermopower since the band structure will remain unaltered. The electrical conductivity though will be affected since the micro-fractures will enhance electronic scattering and consequently increase the electrical resistivity.

The high temperature thermal conductivity behavior of this alloy is extremely interesting (figure 6). The thermal conductivity increases with increasing temperature and the thermal conductivity values for all compositions are very small. The thermal conductivity value for the stoichiometric

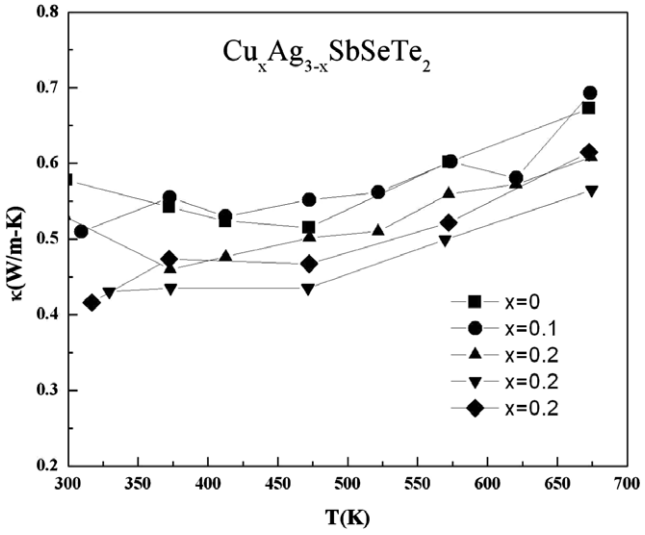


**Figure 6.** High temperature thermal conductivity of $Cu_xAg_{3-x}SbSeTe_2$ for $x = 0$, 0.1 and 0.2.

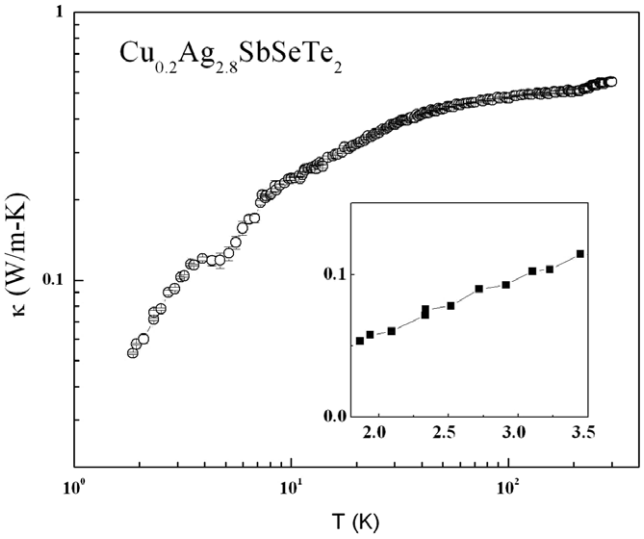


**Figure 7.** Low temperature thermal conductivity $Cu_{0.2}Ag_{2.8}SbSeTe_2$ plotted in log–log scale. The thermal conductivity plateau can be seen at ∼4 K. The inset (linear scale) shows the linear dependence of the thermal conductivity on temperature.

composition ($x = 0$) is $\kappa_{\text{Total}} = 0.67$ W m$^{-1}$ K$^{-1}$ at 700 K while the thermal conductivity value for the $x = 0.1$ alloy is approximately the same. A noticeable decrease is observed for the $x = 0.2$ sample; $\kappa_{\text{Total}} = 0.56$–$0.61$ W m$^{-1}$ K$^{-1}$ at 700 K. The uncertainty in the thermal conductivity values is on the order of 7–8%.

Surprisingly, the low temperature thermal conductivity reveals glass-like behavior (figure 7). According to the x-ray diffraction data, this is a crystalline system so the glass-like behavior is unexpected. The behavior presumably arises due to the large level of disorder which eliminates translational invariance. As a result, heat is transported through localized vibrations and consequently the lattice thermal conductivity is reduced. The presence of localized vibrations typically gives rise to a $\kappa_{\text{Phonon}} \alpha T^2$ dependence of the thermal conductivity at very low temperatures [17–20]. A $\kappa_{\text{Phonon}} \alpha T$ dependence has also been observed at low temperatures in quartz [21, 22] and the bulk-metallic glass [23] $Ni_{59.5}Nb_{33.6}Sn_{6.9}$. In this particular alloy, the low temperature thermal conductivity in the temperature range 1.8 K $\leqslant T \leqslant$ 3.5 K (electronic contribution is negligible in this temperature range) varies linearly with temperature (inset of figure 7). A plateau can also be seen at a temperature $T \sim 4$ K. The appearance of a plateau in the thermal conductivity is a prominent feature of amorphous solids and it is attributed to a rapidly decreasing phonon mean free path with the increasing frequency [24]. At higher temperatures, the increasing thermal conductivity is due to the electronic contribution. The electronic contribution can be calculated using the Wiedemann–Franz law ($\kappa_{\text{electronic}} = LoT/\rho$ with $Lo = 2.45 \times 10^{-8}$ V K$^{-2}$). Using an average value for the resistivity $\rho = 1 \times 10^{-4}$ Ω m we find that the electronic contribution to the thermal conductivity $\kappa_{\text{electronic}} = 0.172$ W m$^{-1}$ K$^{-1}$ which implies that the lattice thermal conductivity is $\kappa_{\text{lattice}} = 0.438$ W m$^{-1}$ K$^{-1}$. The thermal conductivity values for both the stoichiometric and Cu-doped samples, are repeatable and do not vary significantly from sample to sample.

## 4. Conclusions

The electronic and thermal transport behavior of this two-phase alloy make it a good candidate for high temperature thermoelectric applications. The thermopower and thermal conductivity depend very weakly on Cu concentration whereas the resistivity varies considerably. The apparent decoupling of the thermopower, thermal conductivity and resistivity gives us the ability to manipulate the alloy either through slight changes in composition and/or changes in the growth temperature profile, in order to minimize its electrical resistivity (changes in the growth temperature profile did not produce changes in the thermopower and thermal conductivity). Based on our initial measurements ZT values >1.5 are possible. More importantly, we have shown that a phonon glass can be realized in crystalline multi-phase alloys (PGEC) which suggests that multi-phase alloys are important candidates in our search for materials with very high thermoelectric performance.

## Acknowledgments

We would like to thank NSF-DMR-0905322 for the major support of this project. Part of the work at Clemson University is supported from DOE/EPSCoR Implementation Grant (#DE-FG02-04ER-46139), and SC EPSCoR cost sharing. The work at the Los Alamos National Laboratory is supported by the United States Department of Energy.

## References

[1] Tritt T M 2001 *Thermoelectric materials 2000—the Next Generation Materials for Small-Scale Refrigeration and Power Generation Applications: Symp. (San Francisco, CA, April 2000)* (Warrendale, PA: Materials Research Society)

[2] Nolas G S and Materials Research Society 2004 *Thermoelectric Materials 2003—Research and Applications: Symp. (Boston, MA, Dec. 2003)* (Warrendale, PA: Materials Research Society)

[3] Bell L E 2008 *Science* **321** 1457
[4] Venkatasubramanian R, Siivola E, Colpitts T and O'Quinn B 2001 *Nature* **413** 597
[5] Snyder G J and Toberer E S 2008 *Nat. Mater.* **7** 105
[6] Nolas G S, Poon J and Kanatzidis M 2006 *MRS Bull.* **31** 199
[7] Ramazanzade M G, Aliyev S A, Verdiyeva N A and Agayev A M 1981 *Izv. Vyssh. Uchebn. Zaved. Fiz.* **27**
[8] Ferhat M and Nagao J 2000 *J. Appl. Phys.* **88** 813
[9] Lee C, Park Y H and Hashimoto H 2007 *J. Appl. Phys.* **101**
[10] Ma H A, Su T C, Zhu P W, Guo J G and Jia X P 2008 *J. Alloys Compounds* **454** 415
[11] Wang H, Li J F, Zou M M and Sui T 2008 *Appl. Phys. Lett.* **93**
[12] Wojciechowski K, Tobola J, Schmidt M and Zybala R 2008 *J. Phys. Chem. Solids* **69** 2748
[13] Aliev F F, Jafarov M B and Eminova V I 2009 *Semiconductors* **43** 977
[14] Jovovic V and Heremans J P 2009 *J. Electron. Mater.* **38** 1504
[15] Villars P and Calvert L D 1991 *Pearson's Handbook of Crystallographic Data For Intermetallic Phases* (Materials Park, OH: ASM International)
[16] Sugar J D and Medlin D L 2009 *J. Alloys Compounds* **478** 75
[17] Graebner J E, Golding B and Allen L C 1986 *Phys. Rev.* B **34** 5696
[18] Yu C C and Freeman J J 1987 *Phys. Rev.* B **36** 7620
[19] Gil L, Ramos M A, Bringer A and Buchenau U 1993 *Phys. Rev. Lett.* **70** 182
[20] Kuo Y K, Sivakumar K M, Su C A, Ku C N, Lin S T, Kaiser A B, Qiang J B, Wang Q and Dong C 2006 *Phys. Rev.* B **74**
[21] Berman R 1951 *Proc. R. Soc.* A **208** 90
[22] Klemens P G 1951 *Proc. R. Soc.* A **208** 108
[23] Zhou Z H, Uher C, Xu D H, Johnson W L, Gannon W and Aronson M C 2006 *Appl. Phys. Lett.* **89**
[24] Gianno K, Sologubenko A V, Chernikov M A, Ott H R, Fisher I R and Canfield P C 2000 *Phys. Rev.* B **62** 292